

Dynamical scaling law in the development of drift wave turbulence

Takeshi Watanabe and Hirokazu Fujisaka

Department of Physics, Kyushu University 33, Fukuoka 812-81, Japan

Takahiro Iwayama

Department of Control Engineering and Science, Faculty of Computer Science and Systems Engineering, Kyushu Institute of Technology, Iizuka 820, Japan

(Received 8 August 1996)

The Charney-Hasegawa-Mima equation, with random forcing at the narrow band wave-number region, which is set to be slightly larger than the characteristic wave number λ , evaluating the inverse ion Larmor radius in plasma, is numerically studied. It is shown that the Fourier spectrum of the potential vorticity fluctuation in the development of turbulence with an initial condition of quiescent state obeys a dynamic scaling law for $k \ll \lambda$. The dimensional analysis with the assumption that the energy transfer rate ϵ in the inverse cascade is constant with time leads to the scaling form $S(k,t) = \lambda^{1/2} \epsilon^{5/4} t^{7/4} F(k/\bar{k}(t)) [\bar{k}(t) \sim \lambda^{3/4} \epsilon^{-1/8} t^{-3/8}]$ with a scaling function $F(x)$, which turns out to be in good agreement with numerical experiments. [S1063-651X(97)08205-6]

PACS number(s): 47.27.Eq, 52.35.Ra

I. INTRODUCTION

The large scale dynamics of the atmosphere and oceans on the earth or the magnetofluid under the uniform, strong magnetic field are described approximately by the two-dimensional fluid dynamics. The two-dimensional (2D) turbulence has been extensively studied theoretically and numerically since 1960s, and the special properties different from the three-dimensional (3D) turbulence have been clarified. In particular, it is shown that in comparison with the energy cascade theory of the 3D isotropic homogeneous turbulence by Kolmogorov [1], the 2D turbulence generally has two quadratic invariants (the energy and the enstrophy), which makes the existence of the dual cascades possible, i.e., the energy is transported to the small wave-number side (inverse cascade) and the enstrophy is transported to the large wave-number side (direct cascade). This fact yields two types of energy spectra, $E(k) \sim k^{-5/3}$ in the inverse cascade region and $E(k) \sim k^{-3}$ in the direct cascade region [2-4]. As a result the energy is concentrated in large scale eddies in the physical space in the course of time and the self-organization of large scale structure of vortices is observed. These are the important characteristics of the 2D turbulence.

Moreover, direct numerical simulations of the turbulence have been extensively carried out in 1980s and the structure of the physical space in the turbulent field have been attracting researcher's attention. Particularly in the 2D decaying Navier-Stokes (NS) turbulence [5-7], it was proved that the coherent vortices self-organize and stably exist for a long time. In addition these coherent vortices dominate the dynamics of this system, in which vortices with the same sign coagulate each other into larger ones. This dynamical process is closely connected with the energy transfer in the wave-number space.

Recently one of the 2D turbulent systems, the Charney-Hasegawa-Mima (CHM) equation, is studied theoretically [8] and numerically [9,10]. This equation approximately describes the dynamics of the electrostatic field on the plane

perpendicular to the strong magnetic field uniformly applied to plasma [11]. Furthermore, the time evolution of the flow in the geostrophic equilibrium in the planetary atmosphere, which is called the quasigeostrophic potential vorticity equation, is also described by this equation [12]. The CHM equation is written as

$$\frac{\partial}{\partial t}(\nabla^2 \phi - \lambda^2 \phi) + J(\phi, \nabla^2 \phi) = 0, \quad (1)$$

where $\nabla = (\partial/\partial x, \partial/\partial y)$, $J(a,b) = a_x b_y - a_y b_x$. Here $\phi(\mathbf{r}, t)$ denotes the electrostatic potential in plasma or the geostrophic stream function at the position $\mathbf{r} = (x, y)$, and λ is the characteristic wave number representing the ratio of the system size to the ion Larmor radius or the Rossby radius. In the limit of $\lambda \rightarrow 0$, Eq. (1) is reduced to the 2D NS equation. The existence of nonvanishing λ separates Eq. (1) from the 2D NS equation. Equation (1) can be rewritten by operating $(\lambda^2 - \nabla^2)^{-1}$ as

$$\frac{\partial \phi(\mathbf{r}, t)}{\partial t} = \int D(\mathbf{r} - \mathbf{r}') J(\phi(\mathbf{r}', t), \nabla_{\mathbf{r}'}^2 \phi(\mathbf{r}', t)) d\mathbf{r}', \quad (2)$$

$$D(\mathbf{r} - \mathbf{r}') = \frac{1}{(2\pi)^2} \int \frac{e^{i\mathbf{k} \cdot (\mathbf{r} - \mathbf{r}')}}{\lambda^2 + |\mathbf{k}|^2} d\mathbf{k} = \frac{1}{2\pi} K_0(\lambda |\mathbf{r} - \mathbf{r}'|), \quad (3)$$

where $K_0(z)$ is the modified Bessel function of the second kind. Equation (3) stands for the interaction kernel in ϕ field and λ^{-1} represents its interaction range. The interaction range is infinite in the limit of $\lambda \rightarrow 0$, while in the limit of $\lambda \rightarrow \infty$ the interaction becomes local, $D(\mathbf{r} - \mathbf{r}') = \lambda^{-2} \delta(\mathbf{r} - \mathbf{r}')$. In this system, several works have been carried out for the freely decaying turbulence [9] and the forced turbulence [8,10]. It is found that Eq. (1) has the same characteristics as the NS equation for a large wave-number region $k \gg \lambda$ and the statistical law specific of the CHM equation for $k \ll \lambda$. Furthermore, the shell model of the CHM

equation is proposed and studies from the viewpoint of the dynamical systems theory [13] start to be carried out.

The fundamental aim of the present paper is to investigate the formation process of the large scale turbulent fluctuation maintained by the inverse cascade of the energy randomly injected at the narrow band region located at the wave number k_f ($>\lambda$). Especially we aim to study the statistical characteristics of the vortical quasicrystal structure in the case of $k \ll \lambda$ observing the development of the turbulent fluctuation [10].

The paper is organized as follows. In Sec. II we briefly review the scaling law of the energy spectrum in the CHM equation. In Sec. III we present the results of the numerical simulation of the CHM equation with the random forcing at the narrow band wave-number region. Then we derive the scaling law of the structure function of the potential vorticity field in connection with the numerical results. In Sec. IV we briefly discuss the possibility of the intermittency effect on the scaling law and summarize our results.

II. SCALING LAW OF THE ENERGY SPECTRUM IN THE CHM EQUATION

Equation (1) contains two fundamental conserved quantities, the total energy E and the total enstrophy U as

$$E = \frac{1}{L^2} \int [(\nabla \phi)^2 + \lambda^2 \phi^2] d\mathbf{r} = \sum_{\mathbf{k}} (k^2 + \lambda^2) |\phi_{\mathbf{k}}|^2, \quad (4)$$

$$U = \frac{1}{L^2} \int [(\nabla^2 \phi)^2 + \lambda^2 (\nabla \phi)^2] d\mathbf{r} = \sum_{\mathbf{k}} k^2 (k^2 + \lambda^2) |\phi_{\mathbf{k}}|^2, \quad (5)$$

where $\phi_{\mathbf{k}}$ denotes the Fourier component given via $\phi(\mathbf{r}, t) = \sum_{\mathbf{k}} \phi_{\mathbf{k}} e^{i\mathbf{k} \cdot \mathbf{r}}$. The shape of the energy spectrum is formed by the dual cascades of these two conserved quantities; one can obtain the scaling law of the energy spectrum by using the Kolmogorov-type dimensional analysis [8,9].

The equation of motion for $\phi_{\mathbf{k}}(t)$ is written by

$$\frac{d\phi_{\mathbf{k}}}{dt} = -\frac{1}{\lambda^2 + |\mathbf{k}|^2} \sum_{\mathbf{k}'} (\mathbf{k} \times \mathbf{k}')_{\perp} |\mathbf{k} - \mathbf{k}'|^2 \phi_{\mathbf{k}'} \phi_{\mathbf{k} - \mathbf{k}'}. \quad (6)$$

The dimensional analysis yields

$$\phi_{\mathbf{k}} \sim \lambda^2 k^{-4} t^{-1} f(k/\lambda), \quad (7)$$

$$\epsilon \sim \lambda^6 k^{-8} \tau_E^{-3} \tilde{f}(k/\lambda), \quad \eta \sim \lambda^6 k^{-6} \tau_U^{-3} \tilde{f}(k/\lambda), \quad (8)$$

where the energy transfer rate ϵ ($\sim E/t$) and the enstrophy transfer rate η ($\sim U/t$) are assumed to be constant with time, respectively, in the energy cascade region and in the enstrophy cascade region. The times τ_E and τ_U , respectively, represent the energy transfer time scale (eddy turnover time) and the enstrophy transfer time scale. Moreover, $f(x)$ and $\tilde{f}(x)$ ($\equiv (1+x^2)[f(x)]^2$) are dimensionless functions, $f(x)$ being finite for $x \ll 1$ and $f(x) = x^2$ for $x \gg 1$. From Eq. (8), τ_E and τ_U are evaluated as

$$\tau_E \sim \lambda^2 \epsilon^{-1/3} k^{-8/3} g(k/\lambda), \quad \tau_U \sim \lambda^2 \eta^{-1/3} k^{-2} g(k/\lambda), \quad (9)$$

TABLE I. The asymptotic forms of characteristic time scales $\tau_{E,U}$ and the energy spectrum $E(k)$ for different k regions. The upper (lower) part corresponds to $\lambda \ll k_f$ ($k_f \ll \lambda$), k_f being the energy injection wave number. The energy spectrum for $k \ll k_f$ ($k \gg k_f$) is determined by the energy (enstrophy) cascade process.

	$\lambda \ll k_f$		
	$k \ll \lambda$	$\lambda \ll k \ll k_f$	$k_f \ll k$
τ_E	$\lambda^2 \epsilon^{-1/3} k^{-8/3}$		$\epsilon^{-1/3} k^{-2/3}$
τ_U	$\lambda^2 \eta^{-1/3} k^{-2}$		$\eta^{-1/3}$
$E(k)$	$\lambda^2 \epsilon^{2/3} k^{-11/3}$	$\epsilon^{2/3} k^{-5/3}$	$\eta^{2/3} k^{-3}$
	$\lambda \gg k_f$		
	$k \ll k_f$	$k_f \ll k \ll \lambda$	$\lambda \ll k$
τ_E		$\lambda^2 \epsilon^{-1/3} k^{-8/3}$	$\epsilon^{-1/3} k^{-2/3}$
τ_U		$\lambda^2 \eta^{-1/3} k^{-2}$	$\eta^{-1/3}$
$E(k)$	$\lambda^2 \epsilon^{2/3} k^{-11/3}$	$\lambda^2 \eta^{2/3} k^{-5}$	$\eta^{2/3} k^{-3}$

where $g(x) = [\tilde{f}(x)]^{1/3}$. Let k_f be the wave number around which the energy is injected. For $k < k_f$, the process is dominated by the energy transfer, while for $k > k_f$ the enstrophy cascade is dominated. The energy spectrum $E(k)$ defined via $E = \int_0^\infty E(k) dk = \sum_{\mathbf{k}} (k^2 + \lambda^2) |\phi_{\mathbf{k}}|^2$ is, therefore, supposed to be

$$E(k) \sim \lambda^2 \epsilon^{2/3} k^{-11/3} g(k/\lambda) \quad (k < k_f), \quad (10a)$$

$$E(k) \sim \lambda^2 \eta^{2/3} k^{-5} g(k/\lambda) \quad (k > k_f). \quad (10b)$$

In order to determine the asymptotic forms of the above statistical quantities, we consider the following two cases:

$$\lambda \ll k_f, \quad k_f \ll \lambda. \quad (11)$$

It is easy to see that when we consider the case $k \ll \lambda$ in Eq. (6), the λ dependence in the CHM equation is incorporated into the time by putting $t \rightarrow t/\lambda^2$. So the λ dependence of the dynamics does not appear explicitly. The k region under consideration is temporally steady and the energy spectrum has no time dependence. Therefore, the intensity of $\phi_{\mathbf{k}}$ is independent of λ , and $E(k)$ in Eqs. (10a) and (10b) is proportional to λ^2 . The prefactor λ^2 in $E(k)$ comes from the second term in Eq. (4). Consequently, the scaling function $g(x)$ should be finite for $x \rightarrow 0$. On the other hand, for $k \gg \lambda$, the CHM equation has the characteristics of the NS equation, and therefore statistical quantities are independent of λ , which is compatible with the asymptotic form $g(x) = x^2$ ($x \gg 1$). This gives $\tau_{E,U}$ and $E(k)$ quite different from those for $k \ll \lambda$. These results are summarized in Table I.

III. NUMERICAL SIMULATION AND SCALING LAW OF THE STRUCTURE FUNCTION

To investigate the formation process of the turbulent field, we consider the random injection of energy and take the dissipation into account. The CHM equation with a damping term and a forcing term is represented by the Fourier component of ϕ as

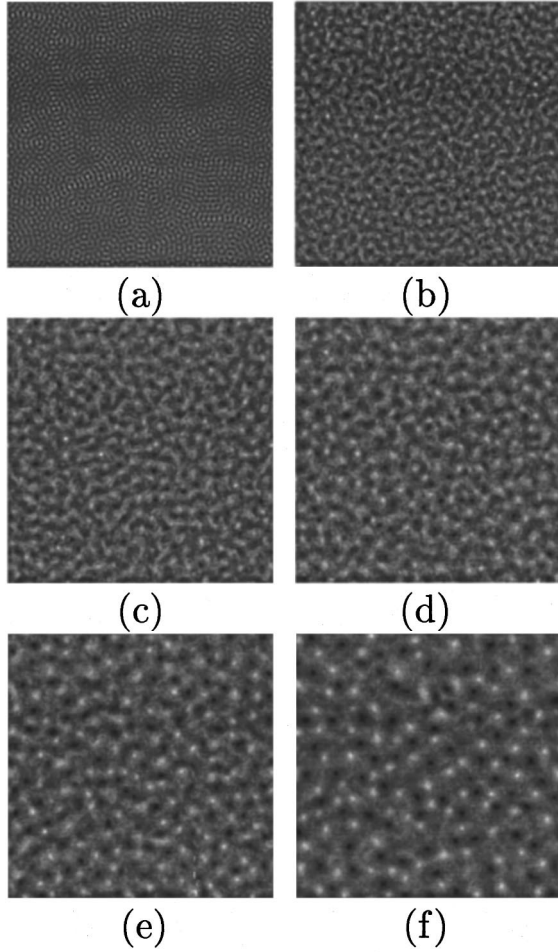


FIG. 1. Snapshots of the potential vorticity field $\xi = \nabla^2 \phi - \lambda^2 \phi$ at (a) $t=2$, (b) 20, (c) 40, (d) 60, (e) 100, (f) 200. White (black) region indicates $\xi > 0$ (< 0).

$$\frac{d\phi_{\mathbf{k}}}{dt} = \frac{1}{\lambda^2 + |\mathbf{k}|^2} \left[- \sum_{\mathbf{k}'} (\mathbf{k} \times \mathbf{k}')_z |\mathbf{k} - \mathbf{k}'|^2 \phi_{\mathbf{k}'} \phi_{\mathbf{k} - \mathbf{k}'} + \nu (|\mathbf{k}|^2)^p (-|\mathbf{k}|^2 \phi_{\mathbf{k}}) + F_e(\mathbf{k}, t) \right]. \quad (12)$$

Here we put the hyperviscosity $p=2$ and $\nu=3.0 \times 10^{-8}$. The system size is fixed as $L=2\pi$, the parameter is put as $\lambda=50$. Moreover, $F_e(\mathbf{k}, t)$ represents the forcing term in the wave-number space applied to the narrow shell of $51 \leq k_f \leq 54$, and therefore $\lambda < k_f$. We consider the form of $F_e(\mathbf{k}, t)$ as $F_e(\mathbf{k}, t) = i(\mathbf{k} \times \mathbf{f}(\mathbf{k}, t))_z$, where the real and imaginary parts of components of $\mathbf{f}(\mathbf{k}, t)$ are chosen to be normal random numbers with the mean value 0 and the variance $\sqrt{0.5}$. The initial condition is chosen such that $\phi_{\mathbf{k}} \approx 0$ which is a random value with small intensity compared with the forcing term and the pseudospectral method [14] is used by dividing the physical space into 256×256 points under the periodic boundary condition. The numerical integration is carried out by using the Runge-Kutta method of the fourth order with the time increment $\Delta t = 2.5 \times 10^{-3}$. We observe the evolution of the potential vorticity $\xi(\mathbf{r}, t) = (\nabla^2 - \lambda^2) \phi(\mathbf{r}, t)$.

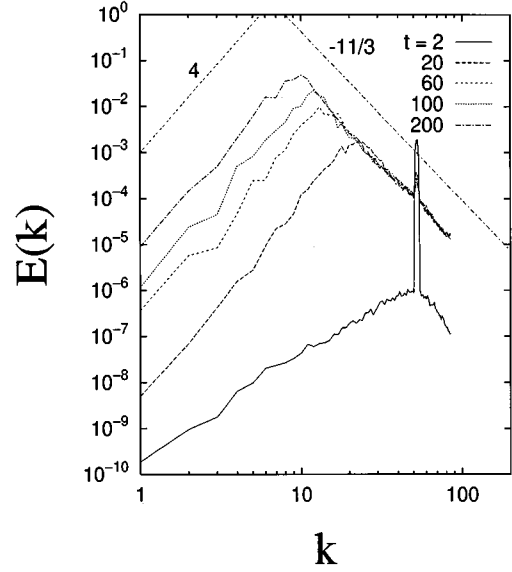


FIG. 2. The time evolution of the energy spectrum $E(k, t)$.

In the process of time evolution, the energy is located in the narrow region around k_f just after the switch on of the forcing, and it is transported to the small wave-number side (the inverse cascade) as well as to the large wave-number region (the direct cascade). The developing process of the turbulent fluctuation is divided into two time regions. In the process of the energy injection the energy spectrum has a single peak structure and its peak position moves to the small wave-number region. If we define the time t_λ when the peak arrives at λ , the coherent vortices being a characteristic of the NS equation are formed during $t < t_\lambda$. The spatial distribution of vortices is at random for $t < t_\lambda$, while they form the quasicrystal structure for $t > t_\lambda$ and the time evolution becomes slow in accordance with that the transport of the energy to the small wave-number side also becomes slow. We define the position of a peak of the energy spectrum at time t as $k_m(t)$, which moves to the small wave-number side. In the time region $\lambda \ll k_m(t) < k_f$ the system dynamics is similar to the NS equation. Then $k_m(t)$ is evaluated as $k_m(t) \sim \epsilon^{-1/2} t^{-3/2}$, provided that we carry out the discussion similar to Eqs. (6)–(9) for $\lambda \rightarrow 0$. The time defined by $\lambda \sim k_m(t_\lambda)$,

$$t_\lambda \sim \epsilon^{-1/3} \lambda^{-2/3}, \quad (13)$$

represents the characteristic time transferring from the behavior of the NS turbulence to the special behavior of the CHM turbulence.

The time evolution of the potential vorticity field is shown in Fig. 1. The figure shows that the peak of the energy localized at k_f in the first time stage moves to the small wave-number side with the increase of the width. This process corresponds to the formation of coherent vortices and the increment of the characteristic length of the system due to the coagulation of vortices. Here t_λ is the time when the peak of the energy spectrum reaches λ . The structure similar to the quasicrystal of the potential vorticity field reported in [10] is observed at $t > t_\lambda$. The time evolution of the energy

spectrum is shown in Fig. 2, which confirms the $k^{-11/3}$ law in the energy inverse cascade region.

To investigate how the typical distance among neighboring vortices with the same sign, the characteristic spatial scale of the system, evolves with time, we observe the structure function $S(k, t)$ of $\xi(\mathbf{r}, t)$ in each time as

$$S(k, t) = \left\langle \left| \int \xi(\mathbf{r}, t) e^{-i\mathbf{k} \cdot \mathbf{r}} d\mathbf{r} \right|^2 \right\rangle, \quad (14)$$

where $\langle \dots \rangle$ denotes the average taken over the orientation of \mathbf{k} . $S(k, t)$ is characterized by the peak height $S_{\max}(t)$ and the characteristic wave-number defined as

$$\bar{k}(t) = \frac{\sum_{k=0}^{\lambda} k S(k, t)}{\sum_{k=0}^{\lambda} S(k, t)}. \quad (15)$$

By noting that $S(k, t)$ has a single peak, the peak position is well approximated by $\bar{k}(t)$. $\bar{k}(t)$ and $S_{\max}(t)$ are plotted as the function of time t in Fig. 3, which asymptotically take the power-law forms

$$\bar{k}(t) \sim t^{-\alpha}, \quad S_{\max}(t) \sim t^{\beta}, \quad (16)$$

where $\alpha \approx 0.37$ and $\beta \approx 1.8$. If $\bar{k}(t)$ is regarded as the peak position of $S(k, t)$, $2\pi/\bar{k}(t)$ evaluates the lattice constant of the quasicrystal structure which is observed for $t \gg t_{\lambda}$.

We can estimate the exponents α and β from the aforementioned Kolmogorov-type dimensional analysis by corresponding the self-organization process of this quasicrystal to the energy inverse cascade process in the Fourier space. We evaluated the eddy turnover time τ_E [Eq. (9)] from the dimensional analysis for the energy transfer rate. This time scale can be regarded as the life time of the eddy with the wave number k . On the other hand, the characteristic wave number k_t of the eddy which disappears at a time t after the start of the injection of the energy is given as $\epsilon \sim \lambda^6 k_t^{-8} t^{-3}$. From this, we can evaluate the time dependence of k_t as

$$k_t \sim \lambda^{3/4} \epsilon^{-1/8} t^{-3/8}. \quad (17)$$

On the other hand, to obtain the asymptote of $S_{\max}(t)$, we use the relation between the energy spectrum $E(k)$ and the structure function $S(k, t)$,

$$E(k, t) = \frac{k S(k, t)}{k^2 + \lambda^2} \quad (18)$$

and Eq. (10a) in the case of $k \ll \lambda$. This combination of Eqs. (10a) and (18) immediately leads to

$$S(k, t) \sim \lambda^4 \epsilon^{2/3} k^{-14/3}. \quad (19)$$

This asymptotic form is valid for $\bar{k}(t) < k \ll \lambda$. The fluctuation in the region $\bar{k}(t) < k \ll \lambda$ is steady because the shape of the structure function in this region does not depend on the time [15].

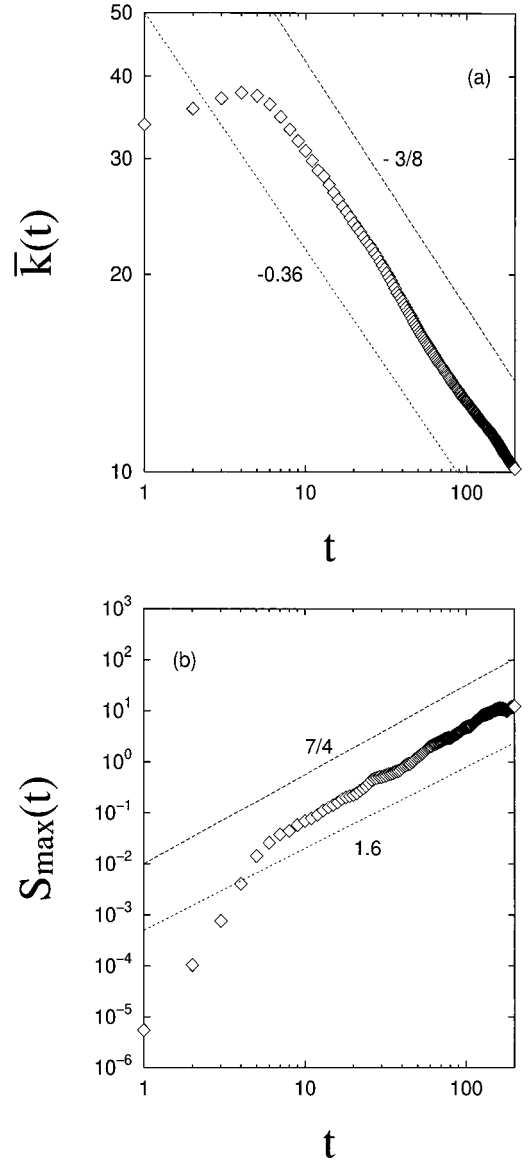


FIG. 3. The time evolution of the characteristic wave number (a) $\bar{k}(t)$ and (b) the peak height $S_{\max}(t)$ of the structure function $S(k, t)$. The slopes $-3/8$ and $7/4$ are the theoretical values with $\theta=0$ and -0.36 and 1.6 denote the values in the case $\theta \approx 0.1$, respectively.

Now, if we suppose that $k_t \sim \bar{k}(t)$ and $S_{\max}(t)$ is replaced by $S[\bar{k}(t)]$, the insertion of Eq. (17) into Eq. (19) yields

$$S_{\max}(t) \sim \lambda^{1/2} \epsilon^{5/4} t^{7/4}. \quad (20)$$

Thus one finds $\alpha = 3/8$ and $\beta = 7/4$, which turn out to be in good agreement with the numerical result (Fig. 3). Furthermore, one should note that the evaluation of t_{λ} [Eq. (13)] is also obtained from Eq. (17) by putting $\lambda \sim \bar{k}(t_{\lambda})$. In order to investigate the temporal evolution of $S(k, t)$, we plot $S(k, t)/S_{\max}(t)$ vs $k/\bar{k}(t)$ for different times in Fig. 4. The figure clearly indicates the existence of the dynamical scaling law as

$$\frac{S(k, t)}{S_{\max}(t)} = F(k/\bar{k}(t)), \quad (21)$$

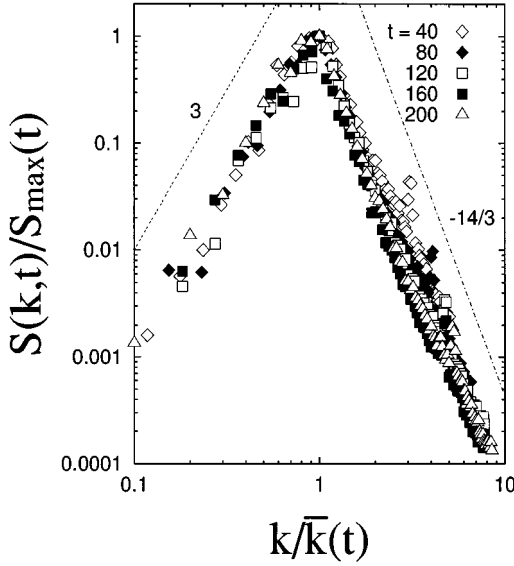


FIG. 4. Scaling plots of $S(k,t)/S_{\max}(t)$ vs $k/\bar{k}(t)$ at $t=40, 80, 120, 160, 200$.

where $F(x)$ is a scaling function [16]. From Fig. 4, the scaling function asymptotically takes the forms

$$F(x) \sim x^{-\gamma} \quad (x > 1), \quad F(x) \sim x^{\delta} \quad (x < 1). \quad (22)$$

The exponent $\gamma = 14/3$ determined from Eq. (19) agrees with the observation in Fig. 4. Since δ is not related to the energy inverse cascade, we have no theory concerning with the determination of δ . Numerical study shows $\delta \sim 3$, which is consistent with the result of the energy spectrum of freely decaying turbulence in the low wave-number region in [9], i.e., $E(k) \sim k^4$.

Finally, let us estimate the Reynolds number Re . In the case $p=2$, the Reynolds number is evaluated by the rate of the nonlinear term and the dissipation term in Eq. (12) as

$$Re \sim \frac{\lambda^{-1} \sqrt{E} l^2}{\nu} \sim t^{5/4}. \quad (23)$$

Here we used $\phi \sim \lambda^{-1} \sqrt{E} \sim t^{1/2}$ (see later) and the characteristic length $l = 2\pi/\bar{k}(t) \sim t^{3/8}$. Therefore, the Reynolds number monotonously increase with time. At $t=200$, we get $Re \sim 10^4$ from Figs. 3 and 5.

IV. DISCUSSION

Until now, we have studied the time evolution of the characteristic spatial scale in the turbulent field from the scaling viewpoint. The scaling law is based on the Kolmogorov-type dimensional analysis with the assumption that the energy transfer rate ϵ is temporally and spatially constant in the energy inverse cascade region. Numerical experiment shows that this is a quite good assumption. Figure 5 shows the time evolution of the energy E per a unit area. If the energy is transferred to the small wave-number side in a constant rate, the energy E is proportional to time ($E \propto t$) because the dissipation is negligible in this region. However Fig. 5 shows the asymptotic form $E \propto t^{1-\theta}$ with a nonvanishing θ in a sufficient time. The excess exponent θ is due to the fluctua-

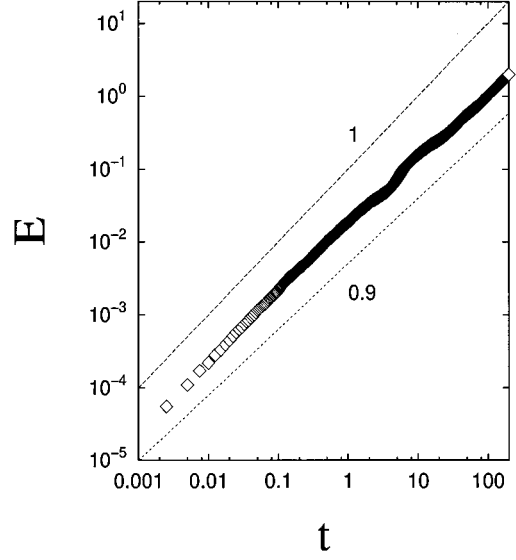


FIG. 5. The time evolution of the energy E per a unit area at $t=0-200$.

tion of the energy transfer rate. The energy injected at k_f is not only transported to the small wave-number side, but also a portion of the energy is transported to the large wave-number region where it is dissipated. Therefore, if the temporal change of the amount of the energy transported to the small wave-number region is random, the fluctuation of the energy transfer rate is observed. It is widely believed that the fluctuation of the energy transfer rate in the 3D turbulence is related to the intermittency of small scale dynamics, consisted of high-vorticity regions and rather low-vorticity (regular) regions in the space [17,18]. In this sense the origin of the fluctuation of the energy transfer rate in the 2D turbulence is different from that in the 3D turbulence.

Without going into the statistical law of the fluctuation of ϵ , we take into consideration the effect of the intermittency phenomenologically by putting $\epsilon \sim t^{-\theta}$. The substitution of this into Eqs. (17) and (20) immediately leads to the modification

$$\bar{k}(t) \sim \lambda^{3/4} t^{-(3-\theta)/8}, \quad S_{\max}(t) \sim \lambda^{1/2} t^{(7-5\theta)/4}. \quad (24)$$

Although the excess exponent θ must be in principle calculated from the CHM equation, if we estimate $\theta \approx 0.1$ from Fig. 5, one gets $\bar{k}(t) \sim t^{-0.36}$ and $S_{\max}(t) \sim t^{1.6}$. Numerical results seem to be compatible with this analysis (Fig. 3).

In the present paper we have investigated the statistical characteristics in the developing process of the turbulent field described by the CHM equation with the random forcing at the narrow band wave-number region. Consequently, we found out the dynamical scaling law as $S(k,t) = \lambda^{1/2} \epsilon^{5/4} t^{7/4} F(k/\bar{k}(t))$, $[\bar{k}(t) \sim \lambda^{3/4} \epsilon^{-1/8} t^{-3/8}]$, using the Kolmogorov-type dimensional analysis, which turned out to be in good agreement with the numerical simulation provided that the energy transfer rate is constant in time. Moreover, we have discussed the revision of the scaling exponents by taking account of the effect of an intermittency as considering the time dependency of the energy transfer rate

$\epsilon \sim t^{-\theta}$. In this connection, we attempt to consider in the case of freely decaying turbulence of the CHM equation. In this case, the energy is almost constant in a long time region. So, if we put $\theta=1$, Eq. (24) yields $\bar{k}(t) \sim t^{-1/4}$, $S_{\max}(t) \sim t^{1/2}$. Here $\bar{k}(t) \sim t^{-1/4}$ has been already derived, e.g., in [9] by using the similarity of the energy spectrum and our other simulation of this case seems to support above results. But the difference between the statistics of the forced turbulence

and the decaying one is quite large, and we must deal with this scaling law more carefully.

ACKNOWLEDGMENTS

T.W. thanks H. Tutu for stimulative discussions. This study was partially supported by Grant-in-Aid for General Scientific Research (No. 40156849) from the Ministry of Education and Culture, Japan.

-
- [1] A. N. Kolmogorov, Dokl. Akad. Nauk USSR **30**, 301 (1941).
 [2] R. H. Kraichnan, Phys. Fluids **10**, 1417 (1967).
 [3] G. K. Batchelor, Phys. Fluids Suppl. **12**, II-233 (1969).
 [4] C. E. Leith, Phys. Fluids **11**, 671 (1968).
 [5] J. C. McWilliams, J. Fluid Mech. **146**, 21 (1984).
 [6] R. Benzi, S. Patarnello, and P. Santangelo, J. Phys. A **21**, 1221 (1988).
 [7] J. C. McWilliams, Phys. Fluids A **2**, 547 (1990).
 [8] M. Ottaviani and J. Krommes, Phys. Rev. Lett. **69**, 2923 (1992).
 [9] V. D. Larichev and J. C. McWilliams, Phys. Fluids A **3**, 938 (1991).
 [10] N. Kukharkin, S. A. Orszag, and V. Yakhot, Phys. Rev. Lett. **75**, 2486 (1995).
 [11] A. Hasegawa and K. Mima, Phys. Fluids **21**, 87 (1978).
 [12] J. Pedlosky, *Geophysical Fluid Dynamics* (Springer-Verlag, New York, 1987).
 [13] J. L. Ottinger and D. Carati, Phys. Rev. E **48**, 2955 (1993).
 [14] S. A. Orszag, Stud. Appl. Math. **100**, 293 (1971).
 [15] Around $k \approx \lambda$, the fluctuation of the potential vorticity is steady in time sufficiently after the peak position $S(k, t)$ passes through $k = \lambda$. We suppose that the structure function at $k \approx \lambda$ satisfies the scaling law
- $$S(k, t) \sim \lambda^4 \epsilon^{2/3} k^{-14/3} h(k/\lambda)$$
- with a scaling function $h(x)$. Note that Eq. (19) is also obtained from this equation by assuming $h(x)$ is finite for $x \ll 1$. The spectrum should be independent of λ for $k \gg \lambda$, which requires that the asymptote $h(x) = x^4$ for $x \gg 1$. This yields $S(k, t) \sim \epsilon^{2/3} k^{-2/3}$, which is consistent with the energy spectrum of the 2D NS equation in the energy inverse cascade region [$E(k) \sim \epsilon^{2/3} k^{-5/3}$].
 [16] Such a scaling law is suggested in the case of freely decaying turbulence of the CHM equation [9].
 [17] F. Anselmet, Y. Gagne, E. J. Hopfinger, and R. A. Antonis, J. Fluid Mech. **140**, 63 (1984).
 [18] G. Paladin and A. Vulpiani, Phys. Rep. **156** (4), 147 (1987).